

Interaction of Separation and Transition in Laminar Separation Bubbles in a 3D-Boundary Layer

T. Hetsch, U. Rist

Institut für Aero- und Gasdynamik,
University of Stuttgart
Pfaffenwaldring 21, 70550 Stuttgart

email: hetsch@iag.uni-stuttgart.de

ABSTRACT:

The influence of different disturbance combinations and increasing sweep on a family of pressure-induced laminar separation bubbles is studied systematically by means of direct numerical simulation (DNS). Three types of disturbance waves are tested against their potential to stimulate the growth of background disturbances of fundamental or subharmonic frequency. The focus is on 2D-disturbances, which are normally the most amplified disturbances in unswept separation bubbles. For the present 3D-base flows, they are found to lose their dominance for sweep angles larger than 10° to 15° . Instead, oblique waves with a propagation direction between 0° and -6° relative to the potential streamline trigger the strongest growth of background disturbances. Spatial linear stability theory (LST) was utilised to select the most amplified disturbances for each sweep angle. LST turned out to be as reliable as in unswept laminar separation bubbles and its excellent agreement with DNS within the linear domain was not adversely affected by the sweep angle.

1.0 INTRODUCTION

1.1 Motivation

Due to strong adverse pressure gradients and low Reynolds numbers, laminar separation bubbles (LSB) are often encountered on high-lift devices of commercial aircraft, on the wings of gliders and smaller unmanned air vehicles. For instance, a laminar separation bubble was measured at the slat of an Airbus A310 in [3]. The corresponding leading-edge sweep angle is $\Psi_\infty=30^\circ$. In the flow regime of incompressible flow with low to moderate Reynolds numbers they are known to strongly influence the performance of airfoils. Although most of the flows of practical interests are inherently 3D, literature about separation bubbles in 3D-flows is rare, and research effort has so far been concentrated almost exclusively on the easier 2D-case. The present work is motivated by the question how much of our knowledge of laminar separation bubbles in a 2D-flow carries over to the swept case and which new phenomena appear. Therefore, the goal of the investigations is two-fold: first, to determine which types of disturbance combinations are effective in swept LSBs in terms of a strong amplification and early transition and second, to study the impact of sweep on the stability and transition of separated 3D-flows. As there is no general theory and nearly no guidance from literature concerning swept laminar separation bubbles, the present study is more qualitative and attempts to formulate some general trends concerning the special situation of LSBs in a swept boundary-layer flow. This should serve as a basis for later investigations and as a first orientation for others new to the field.

1.2 The underlying base flow

A generic family of short leading-edge separation bubbles on a swept plate were calculated by means of direct numerical simulation (DNS). This stationary, purely laminar base flow serves as a basis for the following disturbance calculations and was analysed with spatial linear stability theory (LST) in order to determine the most interesting disturbance combinations. The design is based on previous work on 2D separation bubbles in [4]. The underlying geometry allows a systematic variation of the sweep angle from 0° to 45° . As an example, the whole integration domain including external streamlines and the separating surface of the resulting bubble are shown in figure 1.1 for the 30° -case. The separation bubble itself is created by the introduction of an adverse pressure gradient obtained by prescribing the streamwise velocity component U_e at the upper boundary. An infinite swept flat plate with appropriate pressure distribution is a simple, but suitable, model of a swept wing or high-lift device. A similar setup had been chosen by Horton for his extensive experiments in this field in [1] and [2]. Properties of the swept laminar base flow, the utilised numerical scheme and a first analysis of the effect of sweep by linear stability theory have already been reported in [7]. The strong impact of separation on the amplification rates can exemplarily be seen in figure 1.2, where LST-results of the present 30° separation bubble are compared to a Falkner-Skan-Cooke base flow with the same inflow profiles, but a zero pressure gradient thereafter. The primary instability of the separated flow inside the LSB is up to 16 times stronger.

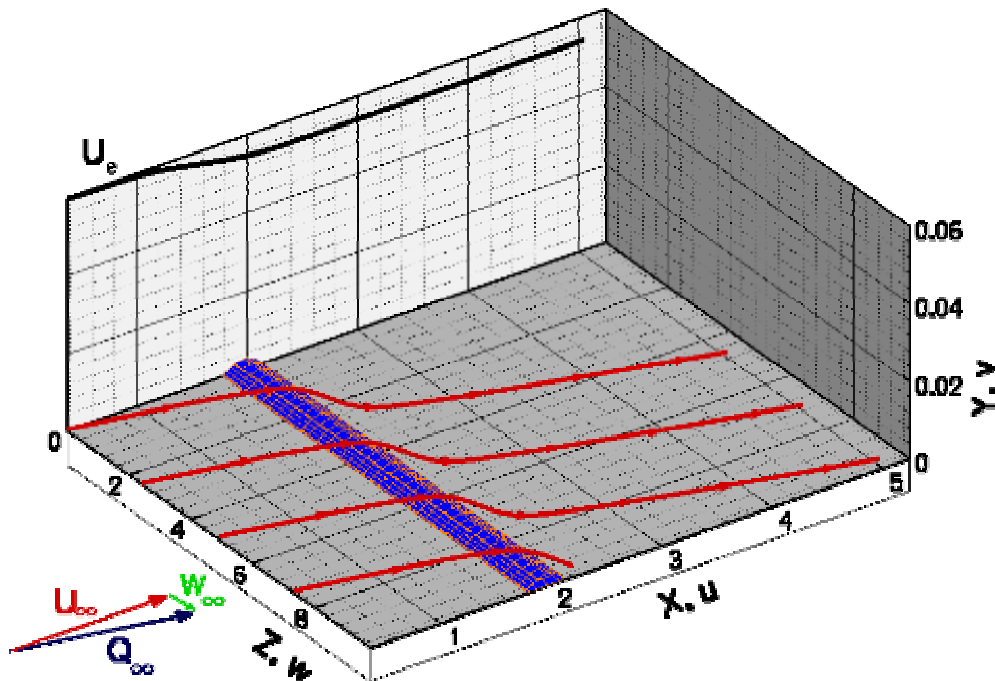


Fig. 1.1: $\Psi_\infty=30^\circ$, base flow with LSB-surface and external streamlines. $U_e(x)$ is the prescribed free-stream velocity in chordwise direction resulting in an adverse pressure gradient.

1.3 Numerical scheme and case parameters

The numerical DNS-scheme is based on the complete incompressible Navier-Stokes-equations in velocity-vorticity formulation and has been successfully applied to 2D-separation bubbles [4] and 3D boundary layer flows [5] in the past. An in-depth description of the 6th-order algorithm can be found in [6]. All quantities are nondimensional, normalised by a reference length $L=0.05\text{m}$, and the chordwise free-stream velocity $U_\infty=30\text{ m/s}$, which was held constant. Different sweep angles Ψ_∞ were realised by varying the spanwise free-stream velocity $W_\infty=U_\infty \cdot \tan(\Psi_\infty)$, as described in [7]. Falkner-Skan-Cooke profiles are

prescribed at the inflow at $x_0=0.37$. The flow is characterised by the Reynolds number $Re_{\delta_1}(x_0) = 331$, based on the displacement thickness at the inflow. All angles are measured relative to the x-axis, the streamwise direction of the unswept case, with positive angles describing clockwise rotation.

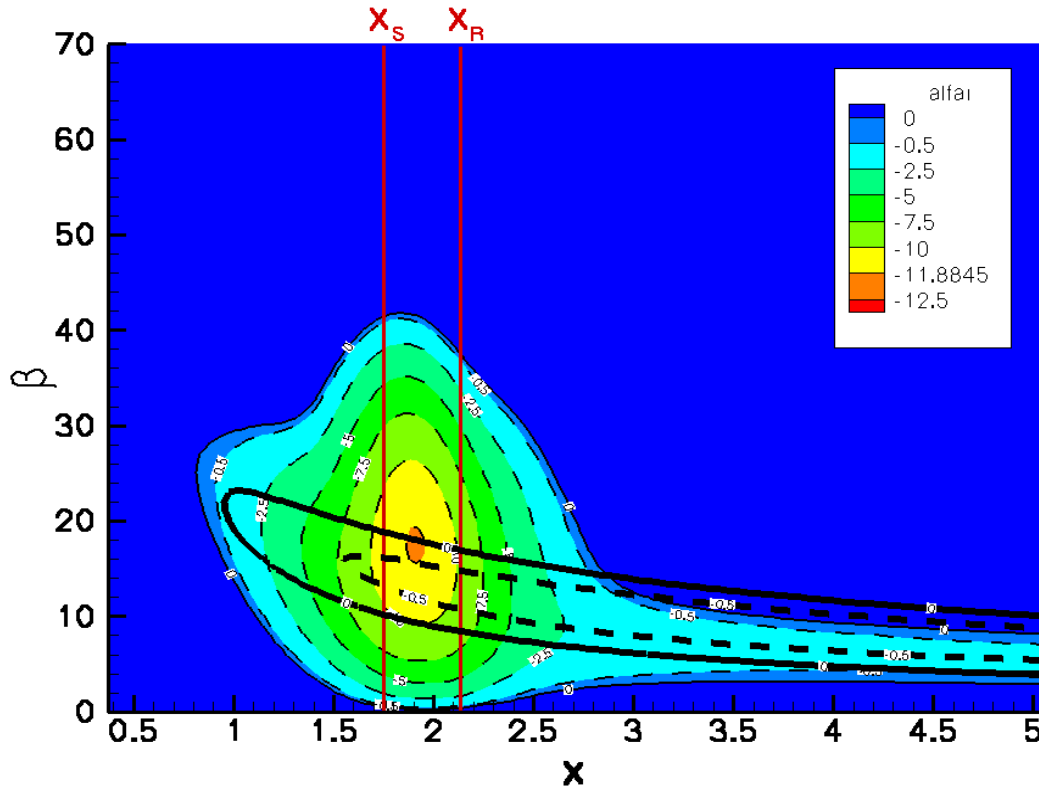


Fig. 1.2: $\Psi_\infty=30^\circ$, comparison of LST-amplification rates α_i of the 30° separation bubble (coloured) and the same base flow without pressure gradient (thick black lines). X_S & X_R = separation & reattachment line.

2.0 DETERMINATION OF THE RELEVANT DISTURBANCE SCENARIOS

2.1 The structure of the disturbance cases

All disturbance calculations follow the same pattern: disturbance waves are excited in the steady, laminar base flow by periodic suction and blowing through the wall. One selected disturbance, the so-called “primary disturbance”, is introduced with a much higher initial v -amplitude of 10^{-5} . Hence the primary disturbance will be dominant throughout the linear and early non-linear regime, defining a certain disturbance scenario. To this disturbance is added always the same set of 17 small “background disturbances” with varying spanwise wave numbers $\gamma \in [-40, -35, \dots, 40]$ as “partners” for non-linear interaction. If the background disturbances, whose initial amplitudes are 5 orders of magnitude lower, share the frequency β with the primary disturbance, we call the scenario a “fundamental” one; else in the case of $\beta/2$ we speak of a “subharmonic case”. This mimics a situation where a single high amplitude disturbance suddenly hits a swept separation bubble in the presence of different background disturbances. Possible resonances and non-linear interactions between them may lead to a much faster breakdown of the laminar state than in the case where only one component is acting. The comparison of figure 2.1 and figure 2.2 shows that the specific choice of the primary disturbance in terms of frequency and spanwise wave number (β/γ) has a noticeable impact on the transition process of the scenario in question.

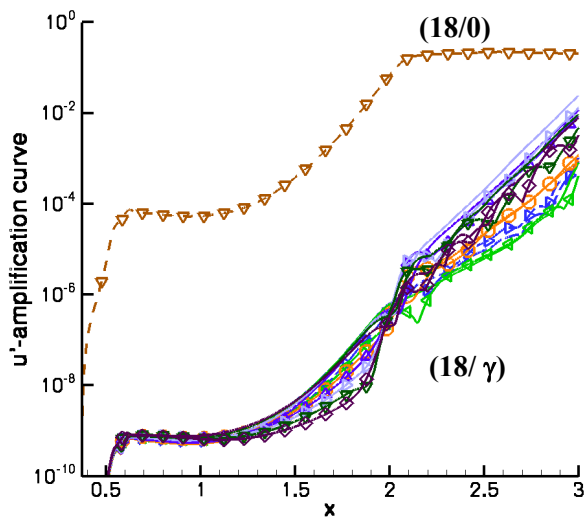


Fig. 2.1: $\Psi_\infty=30^\circ$, fundamental case with a 2D-primary disturbance (18/0).

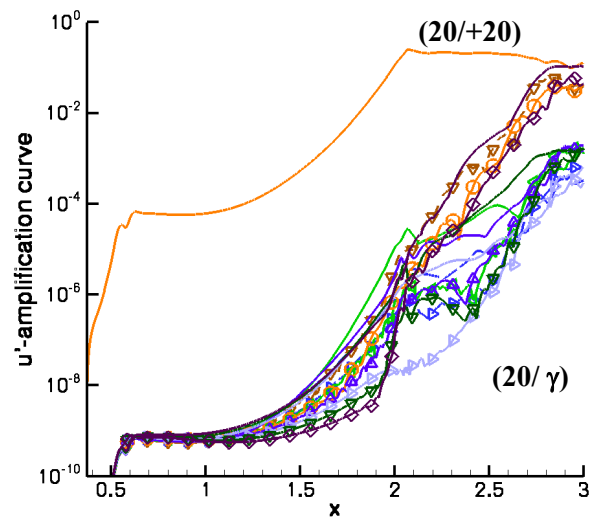


Fig. 2.2: $\Psi_\infty=30^\circ$, fundamental case. Linearly most amplified, oblique primary disturbance (20/+20).

The importance of the primary disturbance becomes obvious when figure 2.1 is compared to a “linear scenario” lacking this disturbance, as in figure 2.3, which can be considered as a reference scenario. The primary instability caused by the swept bubble alone is not strong enough to lift the amplitudes of the extremely small remaining background disturbances to a level of approximately 0.1% to 1% of the free-stream velocity ($U_\infty=1.0$), where non-linear interactions become important. Saturation is not reached. Instead, the disturbances start to decay at the end of the domain and no transition takes place. Therefore, the disturbance growth is purely linear, proved by the generally excellent agreement with the LST-analysis of the undisturbed base flow in figure 2.3, see e.g. the mode (18/+10). Note that the agreement is not spoiled by the sweep angle $\Psi_\infty=30^\circ$ and is only slightly worse for modes like (18/ \pm 40) with large propagation angles of $\Psi \approx 80^\circ$ and $\Psi = -25^\circ$, respectively. Any divergence between LST and DNS in the standard scenarios like in figure 21 is thus a direct measure for the local strength of non-linear effects due to the presence of the primary disturbance: mode interaction, non-linear saturation and non-linear generation of new disturbance modes. As all applied primary modes grow in a similar fashion it makes sense to define a general “linear domain” reaching from $x = 0.9$ to $x = 1.6$ or $x = 1.8$ where the agreement between LST and DNS is very good even in the presence of a primary disturbance.

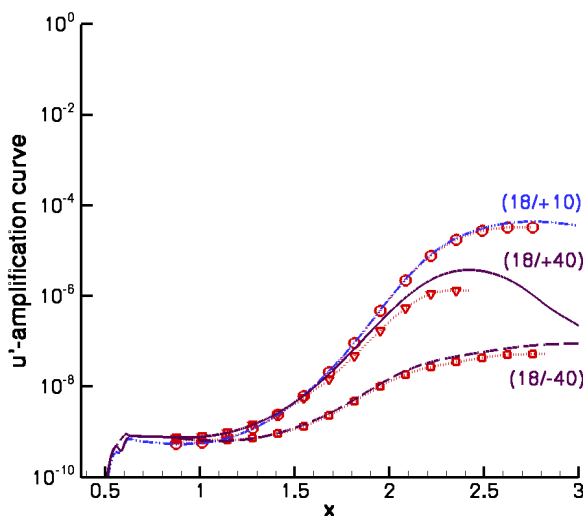


Fig. 2.3: $\Psi_\infty=30^\circ$, linear case. No primary dist. DNS: lines, LST: symbols. All other curves lay between the shown.

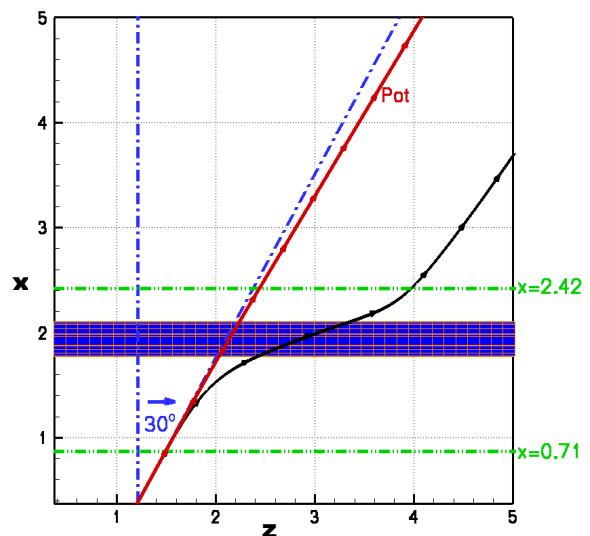


Fig. 2.4: $\Psi_\infty=30^\circ$, bubble-surface, potential streamline, near-wall streamline seen from above.

2.2 Three hypotheses about the fastest road to transition

Our aim is to determine the disturbance combinations (within the concept of section 2.1) most dangerous for the base flow and to study the effect of sweep on them. To this end three hypotheses, illustrated in figure 2.4, are investigated:

Hypotheses: Fastest transition is triggered by primary disturbances which

- i) propagates in 0° -direction along the x -axis (2D-disturbances).
- ii) propagates in direction of the potential streamline.
- iii) experience the strongest overall linear amplification in the swept bubble of their scenario.

All three hypotheses coincide in the 2D-base flow, as the most amplified wave is usually two-dimensional in this case and the potential streamline must follow the 0° -direction by definition. Hypothesis (i) is based on the fact that the pressure gradient caused by the deceleration of the free stream velocity $U_e(x)$ always acts only in the streamwise x -direction. This is a direct consequence of the independence principle of the base flow in an infinite swept-wing geometry. Also, in the unswept case of 2D laminar separation bubbles, 2D-disturbances or weakly oblique modes are the linearly most amplified waves (see [4]). If they remain dominant also in swept base flows, governing the transition process regardless of the sweep angle Ψ_∞ the knowledge of the 2D-case might be helpful for the interpretation of the swept ones and maybe even sufficient for predictions about the behaviour of swept scenarios.

Hypothesis (ii) is motivated by the idea that a swept case should be locally very similar to the 2D-case, if we introduce a coordinate transformation with the direction of the potential streamline as new 0° direction. Because the U_e -deceleration is only moderate and confined to the neighbourhood of the laminar separation bubble ($x \in [0.71; 2.42]$ in figure 2.4) the potential streamline is only slightly curved. As the maximal deviation is only $+2^\circ$ (in the given example of the 30° base flow) the “direction of the potential stream line” and the “sweep angle” are used as synonyms in the following. So we exchange the local transformation for a global one and expect the strongest amplification of a primary disturbance if it propagates approximately in the direction of the sweep angle Ψ_∞ . If (ii) is always true, parts of our knowledge of unswept LSB might be transferable to swept cases by means of the coordinate transformation mentioned above.

Hypothesis (iii) states that the fastest transition to turbulence is to be expected in cases where the primary disturbance reaches the critical level of $1\% U_\infty$ as early as possible, after which it can influence the background disturbances effectively (e.g. by means of resonance). In this case we are to choose the mode with the fastest overall amplification in the linear domain, wherever it may lie in parameter space. LST can be used to identify it for a given scenario. If (iii) is true and if the chosen modes does not appear in a predictable way with growing sweep angle then there is little hope that knowledge of the associated 2D-case might be useful. Each sweep angle would then define a completely new case.

2.3 LST-results for the different sweep angles

For each sweep angle Ψ_∞ and hypothesis in section 2.2, the mode with the strongest integral growth over the linear domain has been chosen by means of LST among all modes fulfilling the condition of the hypothesis in question. There was always a unique maximum in parameter space (β/γ), but neighbouring modes showed nearly identical amplification. Table 2.1 gives an overview:

Ψ_∞	$\Psi=0$	$\Psi=\Psi_\infty$	Ψ	Amp_{max}	Ψ
0°	(18 0)	(18 0)	0°	(18 0)	0°
15°	(18 0)	(18 +10)	12°	(18 +10)	12°
30°	(18 0)	(20 +25)	32°	(20 +20)	25°
45°	(18 0)	(22 +30)	44°	(24 +30)	39°

Table 2.1: Linearly most amplified primary disturbance (β/γ) according to LST with:
 $\Psi=0$: propagation direction 0°
 $\Psi=\Psi_\infty$: propagation in inflow direction
 Amp_{max} : integrally strongest linear amplification
 Ψ : mean local propagation direction

Generally, we see that with increasing sweep angle waves with higher frequency β and spanwise wave number γ experience the strongest growth. It is remarkable that the linearly most amplified mode, which could lay anywhere in parameter space, always propagates roughly in the direction of the potential streamline, with a maximal difference of about 6° in anticlockwise direction in the 45° -case. Therefore, the hypothesis (ii) and (iii) coincide to a certain degree.

3.0 2D-PRIMARY DISTURBANCES AND THE EFFECT OF SWEEP

The following disturbance calculations focus on the influence of primary disturbances on their transition process and on the effect of sweep on the scenarios. To this end the assumptions (i)-(iii) from section 2.2 with their corresponding primary disturbances identified in section 2.3 are compared to each other. The reference cases are the fundamental and subharmonic scenario of the unswept bubble, which has been extensively investigated in [4]. The aim is to find the disturbance combinations with the strongest disturbance amplification and fastest transition to turbulence in a given case, as one expects these to appear in real flows and therefore to be the most relevant for practical applications. In a second step, we want to know how an increasing sweep angle modifies the scenarios. In this way, some general trends concerning the behaviour of the investigated family of swept separation bubbles can be derived. By later comparison with other investigations under different conditions (e.g. much larger separation bubbles with a stronger reverse flow, or different disturbance scenarios like oblique breakdown or white noise) they can be confirmed or modified resulting in a set of “rules of thumb”. After generally understanding swept separation bubbles better, the long-term objective remains to influence and control them.

The cases (ii) and (iii) with oblique primary disturbances show very strong amplification for larger sweep angles and are presently still under investigation. Therefore the main focus is here on the scenarios with 2D-primary disturbances.

3.1 2D primary disturbances (hypothesis (i))

3.1.1 The fundamental case

Figure 3.1 shows the reference case of the unswept bubble as a starting point. After the primary disturbance (18/0) of the 2D-bubble gains sufficient amplitude, it is able to generate, together with the most amplified background disturbance (18/+40), the missing partner (0/-40), thus forming a triad. The identical amplification rates of both background disturbances in figure 3.1 after $x \approx 2.2$ are a sign for resonance. In figure 3.2 we can compare the most amplified background disturbance (18/+40) for each sweep angle Ψ_∞ with the unswept case. Note that the development of the primary disturbance (18/0) there is *independent* of Ψ_∞ , as primary disturbances in our scenarios are generally unaffected by the much smaller background disturbances in the first half of the domain and therefore in perfect agreement with LST nearly to the point of its non-linear saturation, as in figure 3.1. In the special case of $\gamma=0$ however, the influence of the w -velocity component on LST vanishes and only u remains. As a consequence of the independence principle for the base flow, u itself is independent of Ψ_∞ , so that the amplification curves for (18/0) coincide regardless of Ψ_∞ as seen in figure 3.2.

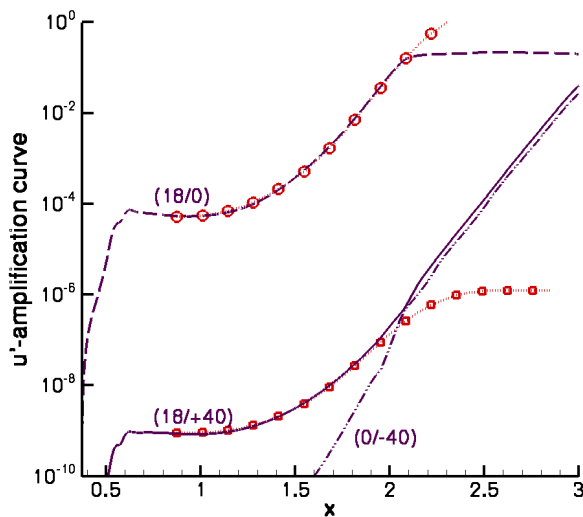


Fig. 3.1: $\Psi_\infty=0^\circ$, fundamental case. 2D-PD (18/0) & (18/+40) form a triad by generating the missing partner (0/-40). Symbols: LST.

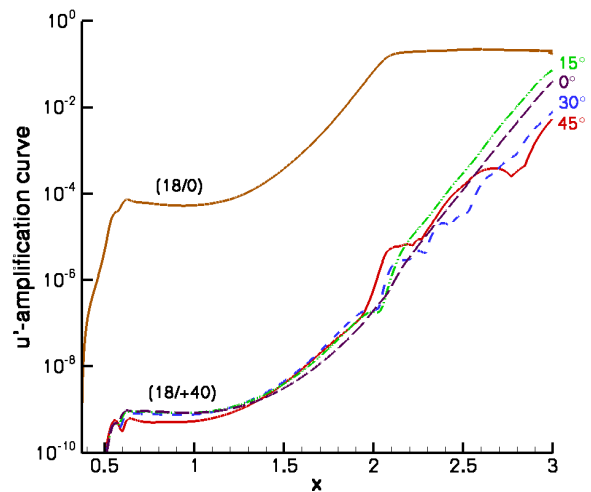


Fig. 3.2: $\Psi_\infty=0^\circ-45^\circ$, fundamental case. 2D-primary disturbance (18/0) and the most amplified background mode (18/+40) for all sweep angles.

Although in the 15° -LSB this mode is a little more amplified and it *locally* exceeds the others in the 45° case at the rear end of the bubble, the general trend is decreasing amplification in the case of rising $\Psi_\infty \geq 15^\circ$. This clearly visible in the complete series of all sweep angles with a 2D primary disturbance in figure 3.3: the local amplification just inside the laminar separation bubble $x \in [x_{sep} = 1.75; x_{reatt} = 2.13]$ increases with growing Ψ_∞ , but globally smaller and smaller amplitude levels are reached.

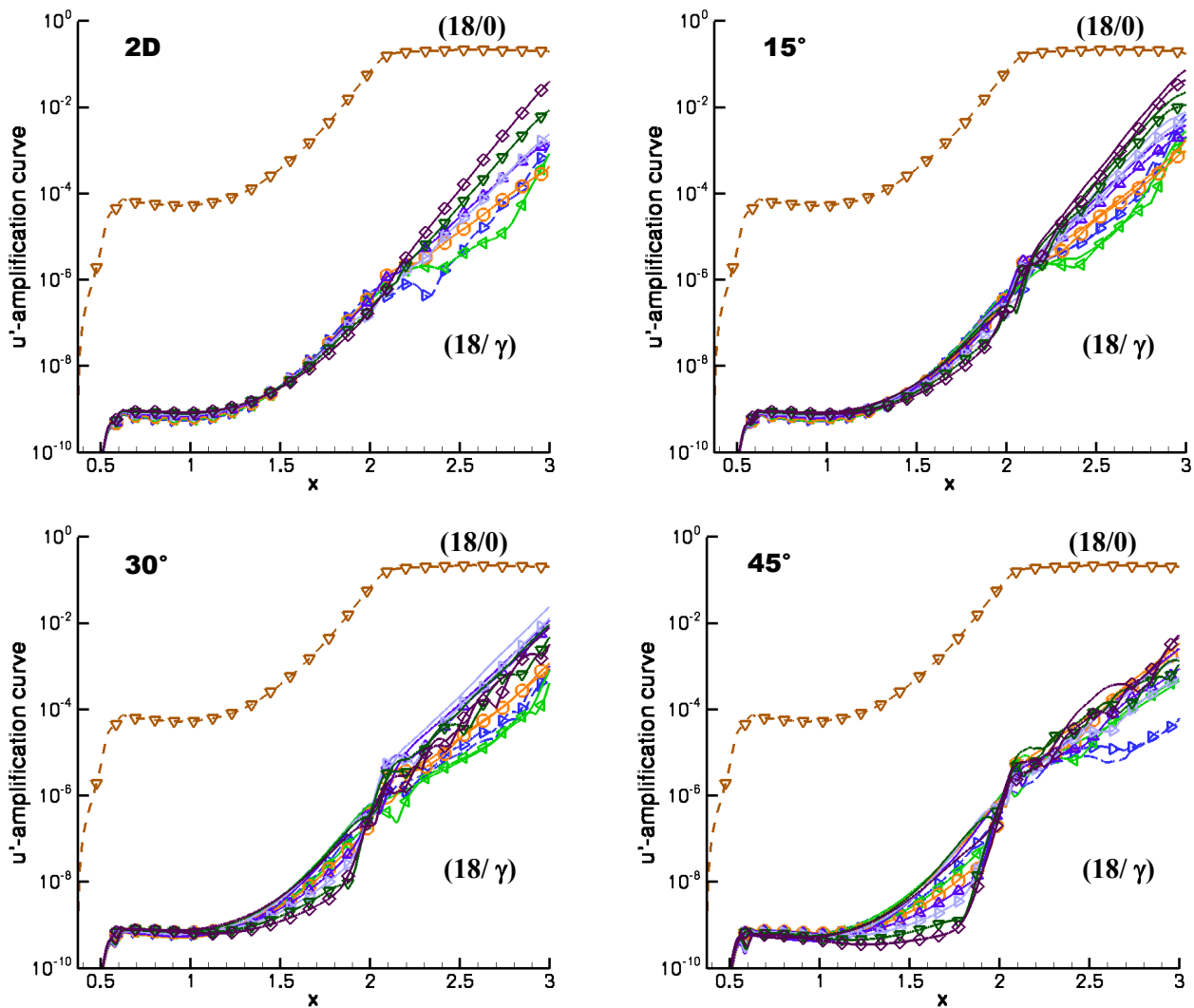


Fig. 3.3: $\Psi_\infty=0^\circ-45^\circ$, fundamental case, all sweep angles: 2D-primary disturbance (18/0) and excited background modes. Although the amplification inside the laminar separation bubble ($x_s=1.75$, $x_r=2.13$) increases with the sweep angle, globally smaller and smaller amplitude levels are reached for $\Psi_\infty>15^\circ$.

It has been shown in [7] that the possible maximal linear amplification is rising with growing sweep angle Ψ_∞ , being e.g. 7% higher in a 45° -base flow compared to the 0° -case at the point of separation $x_{sep}=1.75$. Therefore, slightly more amplified oblique primary disturbances have to exist for the higher sweep angles. This is confirmed in the 30° -base flow of figure 3.4, where the development of the linearly most amplified mode (20/+20) (hypothesis (iii)) and its most amplified triad is compared to the one of the corresponding 2D-primary disturbance (18/0) (hypothesis (i)). More remarkable is the development of the background disturbances due to resonance and non-linear effects: after entering the separation bubble the triad of case (iii) is growing much faster, dominating the 2D-triad by nearly two orders of magnitude and reaching saturation before the end of the domain. This is not the case for small Ψ_∞ which are closer to the unswept situation. In figure 3.5 we see that the primary disturbance (18/+10) (hypotheses (ii) and (iii)) of the 15° -laminar separation bubble experiences virtually the same amplification as the 2D-mode (18/0) and the corresponding background mode (18/+35) grows in the same manner like its 2D-counterpart. So for $\Psi_\infty=15^\circ$ both triads are already equally strongly amplified.

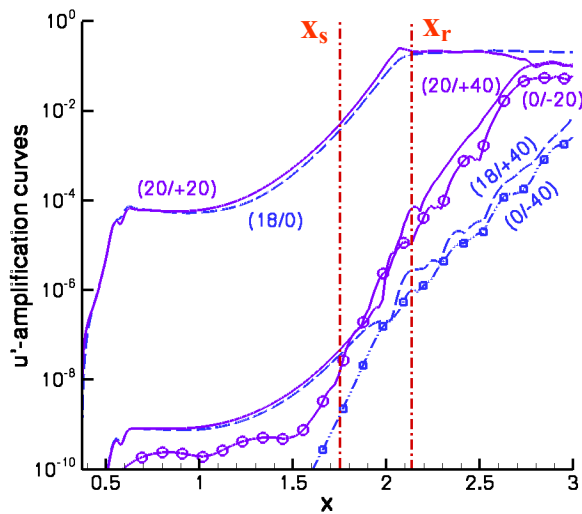


Fig. 3.4: $\Psi_\infty=30^\circ$, fundamental case. 2D-PD (18/0) vs. strongest amplified PD (20/+20) with points of Separation & Reattachment. Symbols: non-linearly generated modes completing the triads.

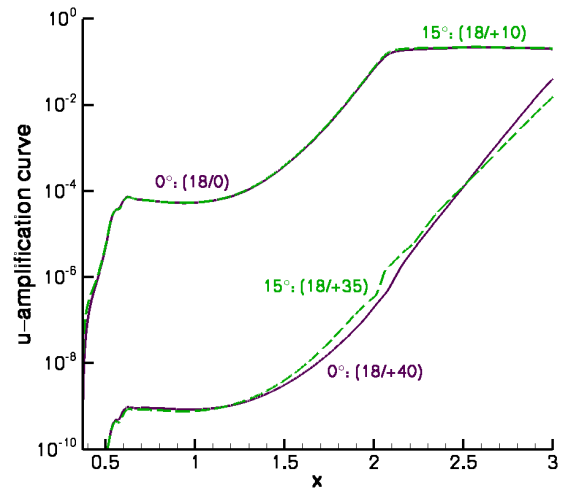


Fig. 3.5: $\Psi_\infty=15^\circ$, fundamental case. 2D-PD (18/0) and linearly strongest amplified PD (18/+10) as well as their background disturbances are already equally strongly amplified at $\Psi_\infty=15^\circ$.

3.1.2 The subharmonic case

The subharmonic case, in which all background disturbances have only half of the frequency of the primary disturbance, exhibits all the trends of the fundamental one, but they appear clearer. As seen in figure 3.6, the most amplified background disturbance (9/+40) simply decreases monotonically with growing sweep angle after reattachment for the case of a 2D-primary disturbance. The comparison with LST in the linear domain works just as well as for the fundamental case. As seen in figure 3.7, also sweep angles as large as $\Psi_\infty=45^\circ$ have no negative effect on the applicability of LST.

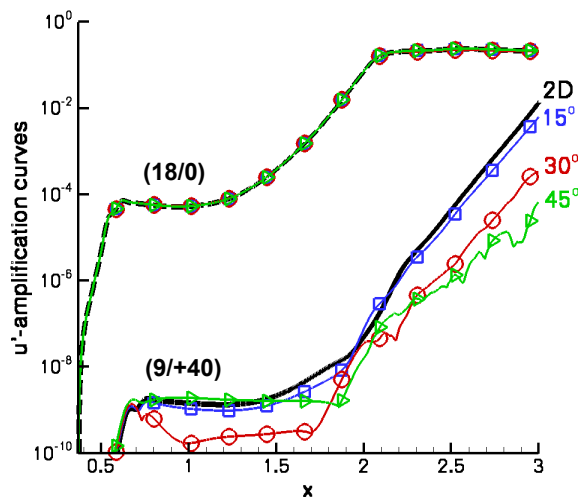


Fig. 3.6: $\Psi_\infty=0^\circ-45^\circ$, subharmonic case. 2D-primary disturbance (18/0) & most amplified background mode (9/+40) compared for all sweep angles.

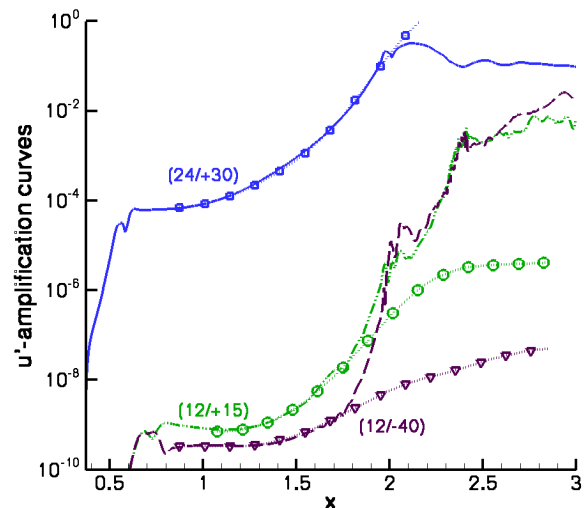


Fig. 3.7: $\Psi_\infty=45^\circ$, subharmonic case. Linearly most amplified PD (24/+30). Rapid growth inside LBS not due to primary instability. Symbols: LST.

Again, there are moderately higher amplified oblique primary disturbances for large sweep angles with an even more pronounced effect on the background disturbances. For the example of the 30° -base flow, figure 3.8 shows that the most amplified triad of hypothesis (iii) exceeds its counterpart of the 2D-primary disturbance by far. A closer look at the same curves normalised with the amplitude level at the neutral point $x=1.1$ in figure 3.9 reveals that the oblique triad surpasses the two-dimensional one by two orders of

magnitude inside the separation bubble ($x=2.0$) and is even more than 1000 times higher at $x=2.5$. Compared to the unswept 2D-base flow, its amplitude level is more than two orders of magnitude greater.

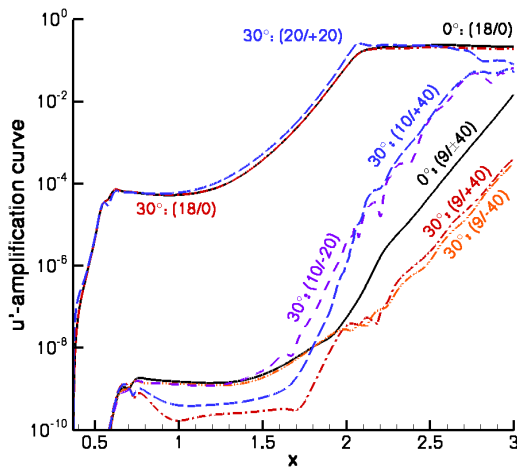


Fig. 3.8: $\Psi_\infty=30^\circ$: subharmonic case. The oblique PD with strongest linear amplification (20/+20) stimulates a much higher amplification of background disturbances than the 2D PD (18/0) in the same base flow or the (18/0) of the unswept case.

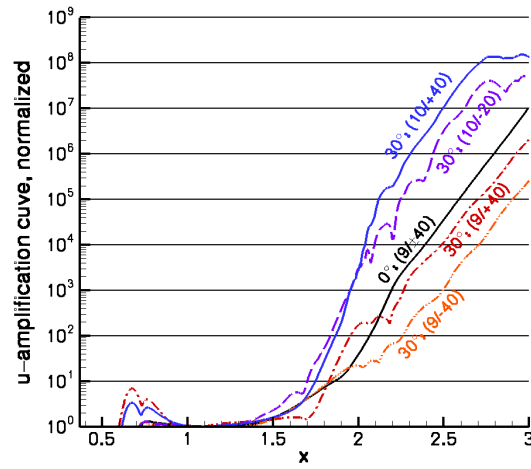


Fig. 3.9: $\Psi_\infty=30^\circ$: subharmonic case. The background disturbances of fig. 3.8 normalised at their neutral point $x=1.1$.

3.1.3 Rejection of hypothesis (i)

As a consequence of the results of the two preceding sections, hypothesis (i) has to be abandoned. Already in the 30° bubble the most amplified triad of the 2D-base flow reaches only 0.1% (subharmonic case) to 1% (fundamental case) of oblique triads, which are even stronger amplified than the 2D-triad in the 2D-baseflow. Neither do the 2D-primary disturbances trigger the fastest road to transition nor is there hope that the knowledge of their behaviour in the unswept case will tell us something useful about the cases with larger sweep angles, where they play only a minor role. A sweep angle of about 15° seems to be the border where oblique modes are becoming equally important. On the other hand, as the change comes gradually, cases with sweep angles of $\Psi_\infty \leq 10^\circ$ can be expected to behave much like the unswept one.

4.0 SUMMARY AND CONCLUSION

Three types of disturbance scenarios have been studied for a series of swept laminar separation bubbles (LSB) with a systematic variation of the sweep angle $\Psi_\infty=0^\circ, 15^\circ, 30^\circ, 45^\circ$. The ability of a single high-amplitude mode, called the primary disturbance, to stimulate the growth of small background disturbances with the same fundamental frequency or the half, subharmonic frequency was investigated with emphasis on 2D primary disturbances. Like in figure 3.8 and 3.9, the specific choice of a primary disturbance in terms of frequency and spanwise wave number can easily result in 100 times higher amplitude levels of the background disturbances. Their importance have been underlined further by comparisons with “linear scenarios” without primary disturbance: the high amplification rates inside the separation bubble are not caused by the primary instability of the base flow. Instead they appear due to resonance and other non-linear effects as a direct consequence of the presence of the primary disturbance.

The focus was on efficiency of two-dimensional modes as primary disturbance (type (i)) in swept flows. For an increasing sweep angle there is an increase of amplification just inside the bubble, but a general decline of the global maximal amplitude level can be observed. In spite of being most effective in the unswept 0° -base flow, for large sweep angles they quickly lose their dominance to oblique modes. At about $\Psi_\infty=15^\circ$ both 2D- and oblique primary disturbances have an equally strong effect. Two oblique

types, the linearly most amplified modes in a given base flow (type (ii)) and primary disturbances propagating in direction of the potential streamline (type (iii)), were also studied. Type (ii) also turned out to propagate always approximately in the same direction with a maximal divergence of -6° for $\Psi_\infty=45^\circ$, so that the types (ii) and (iii) coincide to a certain degree. In an unknown swept laminar separation bubble, a primary disturbances travelling in the direction of the local potential streamline seems therefore to be a promising candidate for maximum background amplification. The types (ii) and (iii) are presently still under investigation, but as a trend they show stronger amplification and earlier transition with increasing sweep angle. In accordance with the unswept case investigated in [4], the subharmonic resonance was generally stronger than in the fundamental case. An exception is the decline of the background disturbances with increasing sweep angle for type (i), which is slower in the fundamental case. 2D-primary disturbances were shown to be relevant only for small sweep angles of $\Psi_\infty \leq 15^\circ$. Clearly investigations of unswept bubbles are insufficient to draw a conclusion about configurations with higher sweep angles.

The quality of spatial linear stability theory (LST) was not affected with increasing sweep angle. The agreement with the DNS-results in the linear domain is as good as in the unswept separation bubbles. Modes with high spanwise wave numbers display a slightly earlier deviation from DNS. The application of LST can therefore also be recommended for swept LSB.

ACKNOWLEDGEMENTS

The financial support by the Deutsche Forschungsgemeinschaft (DFG) under contract number Ri 680/12-1 is gratefully acknowledged.

REFERENCES

- [1] A.D. Young, H.P. Horton (1966): "Some Results of Investigations of Separation Bubbles". AGARD CP-4, pp. 779-811.
- [2] H.P. Horton (1968): "Laminar Separation Bubbles in Two and Three Dimensional Incompressible Flow". PhD thesis, Department of Aeronautical Engineering, Queen Mary College, University of London.
- [3] E. Greff (1991): "In-flight Measurements of Static Pressures and Boundary-Layer State with Integrated Sensors". J. Aircraft, **28**, No.5, pp. 289-299.
- [4] U. Rist (1999): „Zur Instabilität und Transition laminarer Ablöseblasen“. Habilitation, Universität Stuttgart, Shaker Verlag.
- [5] P. Wassermann, M. Kloker (2002): "Mechanisms and passive control of crossflow-vortex-induced transition in a three-dimensional boundary layer". J. Fluid Mech., **456**, pp. 49-84.
- [6] D. Meyer (2003): "Direkte numerische Simulation nichtlinearer Transitionsmechanismen in der Strömungsgrenzschicht einer ebenen Platte". Dissertation, Universität Stuttgart, Shaker Verlag.
- [7] T. Hetsch, U. Rist (2004): "On the Structure and Stability of Three-Dimensional Laminar Separation Bubbles on a Swept Plate". New results in numerical and experimental fluid mechanics IV: Proceedings of the 13. DGLR/STAB-Symposium, Munich, 2002, Breitsamter, Laschka et al. (editors), Notes on Numerical Fluid Mechanics, **87**, Springer Berlin Heidelberg New York.